European Association for the Development of Renewable Energies, Environment and Power Quality (EA4EPQ)

International Conference on Renewable Energies and Power Quality
(ICREPQ'10)
Granada (Spain), 23th to 25th March, 2010

A Direct Power Controller for Doubly-Fed Induction Generator

Alfeu J. Sguarezi Filho and Ernesto Ruppert
DSCE-FEEC-UNICAMP
CEP 13083 - 852 , Caixa Postal 6101 , Campinas - SP, Brasil
sguarezi@dsce.fee.unicamp.br, ruppert@fee.unicamp.br

Abstract - This paper proposes a direct power control scheme for doubly-fed induction generator for variable speed wind power generation. Using a stator flux decoupling and deadbeat control loops the algorithm calculates the rotor voltage vector to be supplied to the rotor in order to eliminate the active and reactive power errors that can achieve high accuracy and fast dynamic power response based on the estimated stator flux, the active and reactive power and their errors. Simulations results are carried out for validation of the digital controller operation.

Keywords - Doubly-fed induction generator, direct power control, wind energy, variable speed constant frequency applications.

I. Introduction

The wind energy systems using a doubly-fed induction generator (DFIG) have some advantages due to variable speed operation and four quadrant active and reactive power capabilities compared with fixed speed induction generators. The stator of DFIG is connected direct to the grid and the rotor links the grid by a bi-directional converter. The rotor converter aims to the DFIG active and reactive power control between the stator and ac supply [1], [2].

Control of DFIG wind turbine systems is traditionally based on either stator-flux-oriented [3] or stator-voltage-oriented [4] vector control. The scheme decouples the rotor current into active and reactive power components. Control of the active and reactive power are achieved with a rotor current controller. Some investigations using PI controllers by using stator-flux-oriented that generates reference currents from active and reactive power errors to the inverter or a cascade PI controllers that generate a rotor voltage which has been presented by [5], [6]. The problem in the use of PI controller is the tuning of the gains and the cross-coupling on DFIG terms in the whole operating range. An interesting method to solve these problems have been presented by [7], [8], [9].

Some investigations by using predictive functional controller [10] and internal mode controller [11], [12] have satisfactory power response when compared with the power response of PI but it is hardly to implement one due to the predictive functional controller and internal mode controller formulation. Another possibility to doubly-fed power control can be made by using fuzzy logic [13], [14]. These strategies have satisfactory power response although it involves relatively complex transformation of voltages, currents and control outputs among the stationary, the rotor and the synchronous reference frames.

The direct power control was applied to the DFIG power control and it has been presented in [15], [16], [17].This scheme calculates the required rotor controlling voltage directly based on the estimated stator flux, active and reactive power and their errors. In [15] the principles and the implementation of DPC is made with hysteresis controllers and variable switching frequency. In [16], [17] the principles of this method are described in detail and simulations results have been presented with variable and constant switching frequency respectively. Moreover, the conventional DPC complicates the AC filter design because of its variable switching frequency. An alternative to direct power control is the power error vector control [18]. This strategy is less complex and obtains similar results to direct power control.

To improve the power response, to eliminate the torque ripple and to protection of rotor-side converter under grid voltage sags a proportional control with anti-jamming control was proposed in [19]. This control has satisfactory power response and eliminate the rotor current overshoot in voltage sags when the loop of torque control is applied, although power and rotor currents results were shown only in fixed speed operation. The proportional controller needs to be carefully tuned to ensure system stability and adequate response within the whole operating range.

The concept of DPC is applied to DFIG under unbalanced grid voltage conditions by [20], [21]. In [20] the active and reactive powers are made to track references using hysteresis controllers. In [21] a notch filter is applied in DPC strategy which allows the power control. These strategies haver satisfactory active and reactive power response under unbalanced grid voltage.

This paper proposes a direct power control scheme that can achieve high accuracy and fast dynamic power response by using a stator flux decoupling and deadbeat control loops. The scheme is derived using a discrete state-space o DFIG model.

The power control aims the active and reactive power control calculates the rotor voltages required to guarantee active and reactive power reach their desired reference values based on the estimated stator flux, the active and reactive power, and their errors. Simulation results are carried out for validation the proposed controller.

II. DFIG Model and DPC

Doubly-fed induction generator model in synchronous reference frame is given by [22]

$$\vec{v}_{1dq} = R_1\vec{i}_{1dq} + \frac{d\vec{\lambda}_{1dq}}{dt} + j\omega_1\vec{\lambda}_{1dq} \quad (1)$$

$$\vec{v}_{2dq} = R_2\vec{i}_{2dq} + \frac{d\vec{\lambda}_{2dq}}{dt} + j\left(\omega_1 - PP\omega_{mec}\right)\vec{\lambda}_{2dq} \quad (2)$$

the relationship between fluxes and currents

$$\vec{\lambda}_{1dq} = L_1\vec{i}_{1dq} + L_M\vec{i}_{2dq} \quad (3)$$

$$\vec{\lambda}_{2dq} = L_M\vec{i}_{1dq} + L_2\vec{i}_{2dq} \quad (4)$$

and generator active and reactive power are

$$P = \frac{3}{2}\left(v_{1d}i_{1d} + v_{1q}i_{1q}\right) \quad (5)$$

$$Q = \frac{3}{2}\left(v_{1q}i_{1d} - v_{1d}i_{1q}\right) \quad (6)$$

The subscripts *1* and *2* represent the stator and rotor parameters respectively, ω_1 is the synchronous speed, ω_{mec} is the machine speed, R_1 and R_2 are the estator and rotor windings per phase electrical resistance, L_1 , L_2 and L_m are the proper and mutual inductances of the stator and rotor windings, $\vec{v}$ is the voltage vector , *PP* is the machine number of pair of poles.

DPC aims independent stator active P and reactive Q power control by means a rotor flux regulation. For this purpose, P and Q are represented as functions of each individual rotor flux. Using stator flux oriented control, that decouples dq axis, (3) and (4) the relationship between stator currents and rotor fluxes is given by

$$i_{2d} = \frac{L_1}{L_1L_2 - L_M^2}\lambda_{2d} - \frac{L_M}{L_1}\frac{L_1}{L_1L_2 - L_M^2}\lambda_1 \quad (7)$$

$$i_{2q} = \frac{L_M}{L_1L_2 - L_M^2}\lambda_{2q} \quad (8)$$

and the active (5) and reactive (6) power can be computed by using Equations (7) and (8)

$$P = -\frac{3v_1L_M}{2\sigma L_1L_2}\lambda_{2q} \quad (9)$$

$$Q = \frac{3v_1L_M}{2\sigma L_1L_2}\left(-\lambda_{2d} + \frac{L_2}{L_M}\lambda_1\right) \quad (10)$$

Equation (2) indicates that the rotor flux change is directly controlled by the applied rotor voltage when rotor resistance is neglected. The components of rotor flux are $\lambda_{2d} = \lambda_2\cos\delta$ and $\lambda_{2q} = \lambda_2\sin\delta$ that can be seen in Figure 1. Thus, rotor fluxes will reflect on stator active and reactive power as can be seen in (9) and (10). Consequently this principle can be used on stator active and reactive power control on rotor side in the DFIG with stator connected to the grid.

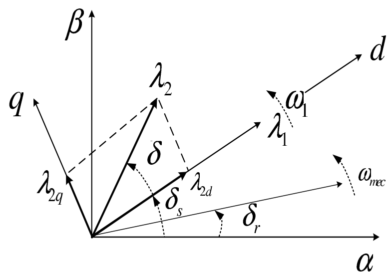

Figure 1. Stator and rotor flux vectors in the synchronous dq frames.

III. Direct Power Control Strategy

Since the applied rotor voltage is also constant during a power control period for voltage-fed PWM and neglecting the rotor resistance, then (2) can be discretized at *k*th sampling instant in synchronous referential frame using the stator flux position and active (9) and reactive (10) power. Thus, the equations that contains only the rotor voltages and power are given by

$$Q(k+1) = \frac{v_{2d}(k)T}{A} + Q(k) + \omega_{sl}P(k)T \quad (11)$$

and

$$P(k{+}1) = \frac{v_{2q}(k)T}{A} + P(k) - \omega_{sl}Q(k)T - \omega_{sl}\frac{L_2}{L_M\,A}\lambda_1 \quad (12)$$

where $\omega_{sl} = \omega_1 - PP\omega_{mec}$, $\sigma = 1 - \frac{L_M^2}{L_1L_2}$ and $A = -\frac{2\sigma L_1L_2}{3v_1L_M}$.

In space state form (11) and (12) become

$$\bar{q}p\left(k+1\right) = A_d\bar{q}p(k) + B_d\bar{v}_2(k) + G_d\bar{\lambda}(k) \quad (13)$$

$$\begin{bmatrix} Q(k+1) \\ P(k+1) \end{bmatrix} = \begin{bmatrix} 1 & \omega_{sl}T \\ -\omega_{sl}T & 1 \end{bmatrix}\begin{bmatrix} Q(k) \\ P(k) \end{bmatrix} + \\ + \begin{bmatrix} \frac{T}{A} & 0 \\ 0 & \frac{T}{A} \end{bmatrix}\begin{bmatrix} v_{2d}(k) \\ v_{2q}(k) \end{bmatrix} + \\ + \begin{bmatrix} 0 & \frac{\omega_{sl}L_2T}{L_M\,A} \\ \frac{-\omega_{sl}L_2T}{L_M\,A} & 0 \end{bmatrix}\begin{bmatrix} \lambda_1(k) \\ 0 \end{bmatrix} \quad (14)$$

From now it will be assumed that the mechanical time constant is much greater then the electrical time constants. Thus $\omega_{mec} = constant$ is a valid approximation for each sample period [23], [24], [25].

A. Decoupling Control

The digital control technique allows to calculate required input to guarantee that the output can achieve high accuracy and fast dynamic response using a discrete equation of the continuous linear system [26], [27], [28].

The rotor voltages $\bar{v}_2$ equations at the $(k-1)$th sampling instant is given by

$$\bar{qp}\,(k) = A_d \bar{qp}(k-1) + B_d \bar{v}_2(k-1) + G_d \bar{\lambda}(k-1) \quad (15)$$

Because $G_d \bar{\lambda}(k)$ and $G_d \bar{\lambda}(k-1)$ are approximately equal, hence, combining (13) and (15) yields an expression which contains only the inputs $\bar{v}_2$ and outputs $\bar{qp}$.

$$\bar{v}_2\,(k) = \bar{v}_2\,(k-1) + B_d^{-1}\{[\bar{qp}(k+1) - \bar{qp}(k)] - A_d[\bar{qp}(k) - \bar{qp}(k-1)]\} \quad (16)$$

Equation (16) indicates that the input can be calculated by using the outputs at the $k-1$, k and $k+1$th sampling instant. This relationship can be used to calculate the input need to procedure the reference at each control instant because both the feedback and the reference at $k-1$ and k sampling period instant are available when (16) is evaluated, either of them can be used in creation of the input.

The control law that uses the reference $\bar{qp}_{ref}$ at the $k+1$ and kth sampling instants to calculate the input $\bar{v}_{2ff}$ can be formulated as

$$\bar{v}_{2ff}\,(k) = \bar{v}_2\,(k-1) + B_d^{-1}[(\bar{qp}_{ref}(k+1) - \bar{qp}(k)) - A_d(\bar{qp}_{ref}(k) - \bar{qp}(k-1))] \quad (17)$$

which means

$$v_{2dff}\,(k) = v_{2d}\,(k-1) + \frac{A}{T}[(Q_{ref}(k+1) - Q(k)) - (Q_{ref}(k) - Q(k-1))] - A\,\omega_{sl}(P_{ref}(k) - P(k-1)) \quad (18)$$

and

$$v_{2qff}\,(k) = v_{2q}\,(k-1) + \frac{A}{T}[(P_{ref}(k+1) - P(k)) - (P_{ref}(k) - P(k-1))] + A\,\omega_{sl}(Q_{ref}(k) - Q(k-1)) \quad (19)$$

where $P_{ref}(k+1)$, $Q_{ref}(k+1)$, $P_{ref}(k)$ and $Q_{ref}(k)$ are the references at $k+1$ and k sampling instant.

The total input applied is given by

$$\bar{v}_{2ref}\,(k) = \bar{v}_{2ff}\,(k) + \bar{v}_{2fb}\,(k) \quad (20)$$

where $\bar{v}_{2fb}$ is achieved making (16)– (17), considering that A_d and B_d is estimated correctly and treating the modeling errors as a disturbance to the output control, then it can be simplified by replacing the output with output errors that is given by

$$\Delta\bar{qp}\,(k+1) = A_d \Delta\bar{qp}\,(k) + B_d \bar{v}_{2fb}\,(k) \quad (21)$$

where $\Delta\bar{qp}\,(k) = \bar{qp}_{ref}\,(k) - \bar{qp}\,(k)$. Note that when realizing the control, $\bar{qp}_{ref}(k+1)$ is not available at the time when $\bar{v}_{2ff}$ is calculated. Therefore, $\bar{qp}_{ref}(k)$ must be used instead $\bar{qp}_{ref}(k+1)$. In essence, the control reference must be delayed one sampling period in the control. The effect of delaying the reference one sampling period will shift the output response back one sampling period as well, but the shape of the output response remains the same.

B. Deadbeat Feedback Control

To achieve a fast output response and a null steady state error a separate feedback control is made by using (21) and making $\bar{v}_{2fb}\,(k) = -G_c \Delta\bar{qp}\,(k)$. One is given by

$$\Delta\bar{qp}\,(k+1) = (A_d - B_d G_c)\,\Delta\bar{qp}\,(k) \quad (22)$$

From (22) the gains required to null steady state error are found by $(A_d - B_d G_c) = 0$. Thus, G_c is given by

$$G_c = A\left(\frac{1}{T} - j\omega_{sl}\right) \quad (23)$$

The block diagram representing (17) and (22) is shown in Figure 2.

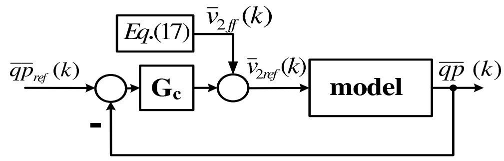

Figure 2. Decoupling and deadbeat control block diagram.

The DPC control scheme uses a digital controller to obtain rotor voltages which should be applied on generator in order to guarantee active and reactive power reach their desired reference values, the method directly calculates required rotor control voltage with each switching period, based on the estimated stator flux, the active and reactive power, and their errors. The power control block diagram is shown in Figure 3. The converter that is connected to the grid control the voltage of the link DC and one can be controlled by using any control presented in [29].

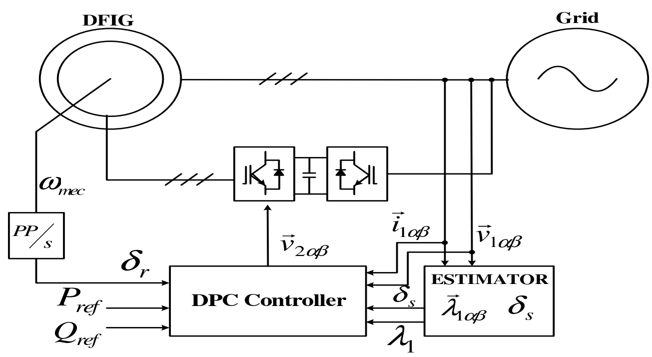

Figure 3. DPC block diagram.

Thus, if the d and q axis voltage components are calculated according (18), (19), (20) and (23) above are applied to the generator, then the active and reactive power convergence to their respective commanded values will occur. The desired rotor voltage in the rotor $\alpha\beta$ reference frame generates switching signals for the rotor side using either space vector modulation that is given by $v_{2\alpha\beta} = v_{2dq}\, e^{\delta_s - \delta_r}$.

Stator currents and voltages, rotor speed and currents are measured to stator flux position δ_s and magnitude λ_1, synchronous frequency ω_1 and slip frequency ω_{sl} estimation.

C. *Estimation*

To digital power control is required to calculate the active and reactive power values, their errors, the stator flux magnitude and position, the slip speed and synchronous frequency.

The flux estimation using (1) is given by

$$\vec{\lambda}_{1\alpha\beta} = \int \left(\vec{v}_{1\alpha\beta} - R_1 \vec{i}_{1\alpha\beta} \right) dt \tag{24}$$

and the flux position by using equation (24) as

$$\delta_s = \arctan \left(\frac{\lambda_{1\beta}}{\lambda_{1\alpha}} \right) \tag{25}$$

The synchronous speed ω_1 estimation is given by

$$\omega_1 = \frac{d\delta_s}{dt} = \frac{(v_{1\beta} - R_1 i_{1\beta})\, \lambda_{1\alpha} - (v_{1\alpha} - R_1 i_{1\alpha})\, \lambda_{1\beta}}{(\lambda_{1\alpha})^2 + (\lambda_{1\beta})^2} \tag{26}$$

and the slip speed estimation by using the rotor speed and synchronous speed is

$$\omega_{sl} = \omega_1 - PP\omega_{mec} \tag{27}$$

The angle in rotor stationary reference frame is given by

$$\delta_s - \delta_r = \int \omega_{sl} dt \tag{28}$$

IV. Simulation Results

In the simulation of proposed digital control strategy was used MATLAB/SimPowerSystems®package. The digital power control strategy has a $T = 10^{-4} s$ and the DFIG parameters are shown in Appendix. Figure 3 shows the schematic of the implemented system. To the power factor (PF) control the reactive power reference is given by

$$Q_{ref} = P_{ref} \frac{\sqrt{1 - PF^2}}{PF}$$

Initial studies with various active and reactive power steps and constant rotor speed at 226.6 rad/s were carried out to test the dynamic response of the proposed power control strategy are shown in Figure 4. The initial active power and power factor references were being -50 kW and FP=+0.85. The active power and power factor references were step changed from -60 to -100 kW and from PF of 0.85 to -0.85 at 0.25 s and the power reference were step changed again from -100 to -149.2 kW and from PF of -0.85 to 1 at 0.5 s, respectively. The rotor and stator currents and the rotor speed are shown in Figure 5. The dynamic response of both active and reactive power are in few milliseconds, there is no overshoot of either stator/rotor or the active/reactive power and the satisfactory performance and robustness of the controller can be seen.

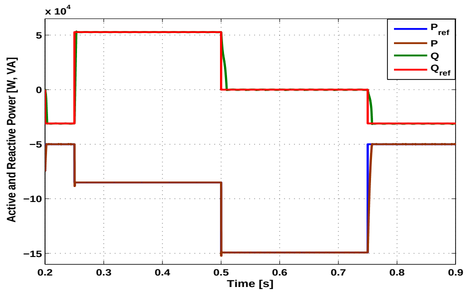

Figure 4. Response of step tests for active and reactive power and rotor currents in supersynchronous operation.

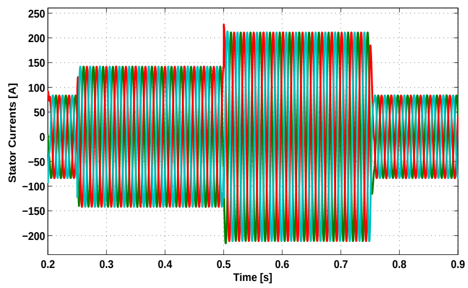

(a) Stator Currents.

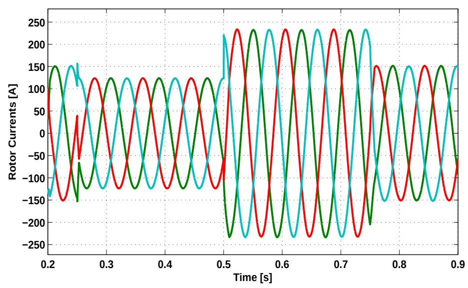

(b) Rotor Currents.

Figure 5. Stator and rotor currents and rotor speed in supersynchronous operation.

Studies with various power steps and rotor speed were carried out to further test the proposed power control schemes. During the period 0.25-0.6 s, the rotor speed increased from 151.1 rad/s to 226.6 rad/s. The Figure 6 shows the results step reference tests of active and reactive power. The power steps, i.e., active power and power factor references were changed from -60 to -100 kW and from PF of 0.85 to -0.85 at 0.25 s. The rotor current and speed and stator current are shown in Figure 7.

To test the impact of the parameters variations on the system performance the rotor resistance R_2 and mutual inductance L_M are increased of 20%. The same tests of step reference of active and reactive power with rotor speed variation and with parameters variation are shown in Figures 8 and 9. Comparing Figures 6 and 8 and Figures 7 and 9, there is hardly any difference, and even with such large inductance and rotor resistance errors, the system maintains satisfactory performance under both steady-state and transient conditions.

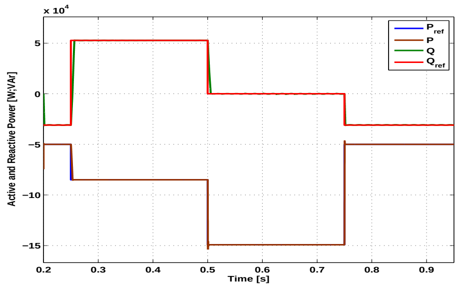

Figure 6. Response of step tests for active and reactive power in several speed operation.

V. Conclusion

This paper has presented a DPC by using stator flux decoupling and deadbeat controllers for doubly fed induction generator that can achieve high accuracy and fast dynamic power response. The controller uses the DFIG equations to calculate the required rotor voltages in order to the active and the reactive power values reach the desired reference. The power control scheme helps the protection of rotor-side converter because there is no overshoot in the rotor current. Constant converter switching frequency is achieved that eases the design of the power converter and the ac harmonic filter. The impact of machine parameters variations is analyzed and found to be negligible due to the fact that in the deadbeat controller formulation the model errors was treated as a disturbance to the output control. The simulations confirm the effectiveness and the robustness of the DPC during several operating conditions and variations of machine parameters.

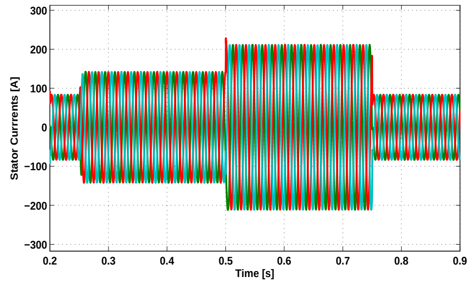

(a) Stator Currents.

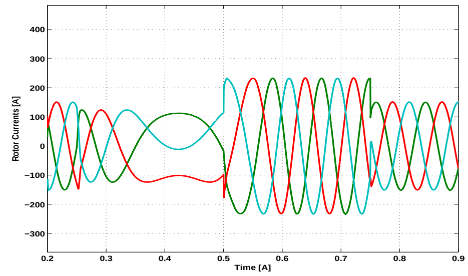

(b) Rotor Currents.

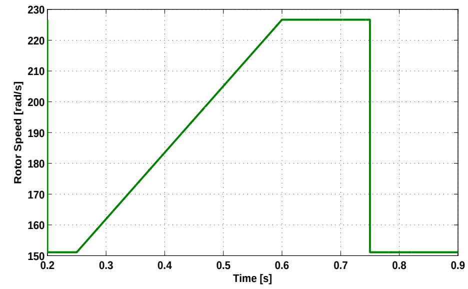

(c) Rotor Speed.

Figure 7. Stator and rotor currents and rotor speed in several speed operation.

References

[1] M. G. Simões and F. A. Farret, *Renewable Energy Systems with Induction Generators*. CRC PRESS, 2004.

[2] R. Datta and V. T. Rangathan, "Variable-speed wind power generation using doubly fed wound rotor induction machine - a comparison with alternative schemes," *IEEE Trans. on Energy Conversion*, vol. 17, no. 3, pp. 414–421, September 2002.

[3] B. H. Chowdhury and S. Chellapilla, "Double-fed induction generation control for variable speed wind power generation," *Electric Power System Research*, no. 76, pp. 786–800, 2006.

[4] B.Hopfensperger, D.J.Atkinson, and R. Lakin, "Stator-f lux-oriented control of a doubly-fed induction machine with and without position encoder," *IEE Proc.-Electr. Power Applications*, vol. 147, no. 4, pp. 241–250, April 2000.

[5] A. Tapia, G. Tapia, J. X. Ostolaza, and J. R. Sáenz, "Modeling and control of a wind turbine driven doubly fed induction generator," *IEEE Trans. on Energy Conversion*, no. 194-204, June 2003.

[6] R. V. Jacomini, "Power flux control of doubly fed induction generator operating at sub-synchronous speeds," School of Electrical and Computer Engineering,Unicamp University of Campinas, Master Degree Thesis, August 2008.

[7] J. P. da Costa, J. Marques, H. A. Gründling, and H. Pinheiro, "Dynamic behavior of the doubly-fed induction generator in stator flux vector reference frame," *Eletrônica de Potência*, vol. 13, no. 1, pp. 33–42, March 2006.

[8] R. G. de Oliveira, J. L. da Silva, and S. R. Silva, "Development of a new reactive power control strategy in doubly-fed induction generators for wind turbines," *Eletrônica de Potência*, vol. 13, no. 4, pp. 277–284, November 2008.

[9] F. P. anb T. Bouaouiche and M. Machmoum, "Advanced control of a doubly-fed induction generator for wind energy conversion," *Electric Power Systems Research*, vol. 79, pp. 1085 –1096, 2009.

[10] Z. Xin-fang, X. Da-ping, and L. Yi-bing, "Predictive functional control of a doubly fed induction generator for variable speed wind turbines," *IEEE World Congress on Intelligent Control and Automation*, June 2004.

[11] J. Morren and M. Sjoerd W. H. de Haan, "Ridethrough of wind turbines with doubly-fed induction generator during a voltage dip," *IEEE Transactions on Energy Conversion*, vol. 20, no. 2, pp. 435–441, June

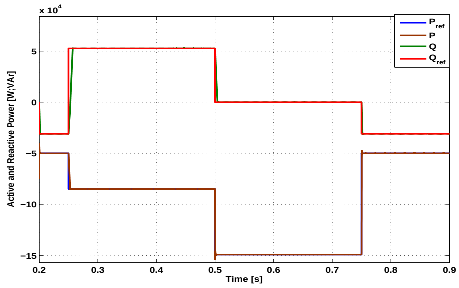

Figure 8. Response of step tests for active and reactive power with parameters variations in several speed operation.

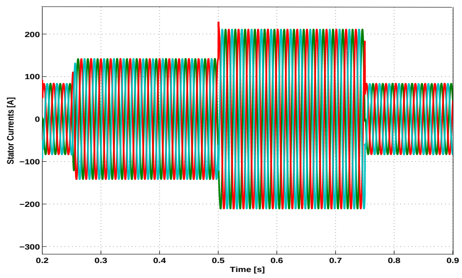

(a) Stator Currents.

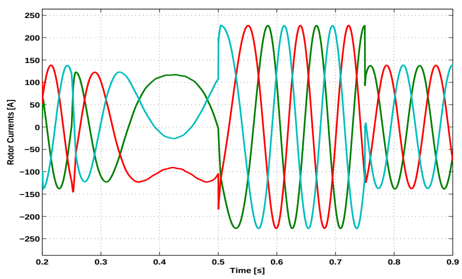

(b) Rotor Currents.

Figure 9. Stator and rotor currents with in several speed operation and with parameters variations.

2005.

[12] J. Guo, X. Cai, and Y. Gong, "Decoupled control of active and reactive power for a grid-connected doubly-fed induction generator," *Third International Conference on Electric Utility Deregulation and Restructuring and Power Technologies. DRPT 2008.*, pp. 2620 – 2625, April 2008.

[13] J. P. A. V. anb Marcus Vinicius Alves Nunes, U. H. Bezerra, and A. C. do Nascimento, "Controladores fuzzy aplicados ao conversor de geradores de indução duplamente excitados em sistemas eólicos integrados a sistemas de potência," *Revista Controle & Automação*, vol. 18, no. 1, pp. 115–126, Jan., Feb., March 2007.

[14] X. Yao, Y. Jing, and Z. Xing, "Direct torque control of a doubly-fed wind generator based on grey-fuzzy logic," *International Conference on Mechatronics and Automation. ICMA 2007.*, pp. 3587 – 3592, August 2007.

[15] R. Datta and V. T. Ranganathan, "Direct power control of grid-connected wound rotor induction machine without rotor position sensors," *IEEE Transactions on Power Electronics*, vol. 16, no. 3, pp. 390 – 399, May 2001.

[16] L. Xu and P. Cartwright, "Direct active and reactive power control of dfig for wind energy generation," *IEEE Trans. on Energy Conversion*, vol. 21, no. 3, pp. 750–758, September 2006.

[17] D. Zhi and L. Xu, "Direct power control of dfig with constant switching frequency and improved transient performance," *IEEE Trans. on Energy Conversion*, vol. 22, no. 1, pp. 110–118, March 2007.

[18] I. de Alegria, J. Andreu, P. Ibanez, J. L. Villate, and I. Gabiola, "Novel power error vector control for wind turbine with doubly fed induction generator," *Industrial Electronics Society, 2004. IECON 2004. 30th Annual Conference of IEEE*, vol. 2, pp. 1218–1223, November 2004.

[19] G. Xiao-Ming, S. Dan, H. Ben-Teng, and H. Ling-Ling, "Direct power control for wind-turbine driven doubly-fed induction generator with constant switch frequency," *International Conference on Electrical Machines and Systems*, pp. 253–258, October 2007.

[20] D. Santos-Martin, J. L. Rodriguez-Amenedo, and S. Arnalte, "Direct power control applied to doubly fed induction generator under unbalanced grid voltage conditions," *IEEE Transactions on Power Electronics*, vol. 13, no. 5, pp. 115–126, September 2008.

[21] D. Sun, X. Guo, L. Shang, and Y. He, "Modified dpc for dfig based wind power generation under unbalanced grid-voltage," *International Conference on Electrical Machines and Systems. ICEMS 2008.*, pp. 2299–2304, October 2008.

[22] W. Leonhard, *Control of Electrical Drives*. Springer-Verlag Berlin Heidelberg New York Tokyo, 1985.

[23] S. Yamamura, *Spiral Vector Theory of AC Circuits and Machines*. Clarendon Press OXFORD, 1992.

[24] F. Briz, M. W. degener, and R. D. Lorenz, "Analysis and design of current regulators usin complex vectors," *IEEE Trans. Ind. Applicat.*, vol. 32, pp. 817–825, May-June 2000.

[25] J. Holtz, J. Quan, J. Pontt, J. Rodríguez, P. newman, and H. Miranda, "Design of fast and robust current regulators for high-power drives based on complex state variables," *IEEE Trans. Ind. Applications*, vol. 40, pp. 1388–1397, September/October 2004.

[26] G. F. Franklin, J. D. Powel, and M. l. Workman, *Digital Control of Dynamic Systems*. Addison-Wesley Publishing Company, 1994.

[27] S.-M. Yang and C.-H. Lee, "A deadbeat current controller for field oriented induction motor drives," *IEEE Trans. on Power Electronics*, vol. 17, no. 5, pp. 772–778, 2002.

[28] A. J. S. Filho, M. de Oliveira Filho, and E. R. Filho, "A digital active and reactive power control for doubly-fed induction generetator," *IEEE Power Electronics Specialists Conference, PESC 2008.*, pp. 2718 – 2722, June 2008.

[29] J. R. Rodríguez, J. W. Dixon, J. R. Espinoza, J. Pontt, and P. Lezana, "Pwm regenerative rectifiers: State of the art," *IEEE Trans. Ind. Electronics*, vol. 52, no. 1, February 2005.

APPENDIX

Doubly-fed induction generator parameters $R_1 = 0.02475$ Ω; $R_2 = 0.0133$ Ω; $L_m = 0.01425$ H; $L_{l1} = 0.000284$ H; $L_{l2} = 0.000284$ H; $J = 2.6$ $Kg \cdot m^2$; $PP = 2$; $PN = 149.2$ kVA; $V_N = 575$ V.